Numerical Investigations of Aerodynamic Characteristics Prediction of High-lift Low Reynolds Number Airfoil

Smail Boughou[1*], Ashraf A. Omar[1], Omer A. Elsyed[1], Mohammed Aldheeb[2]

[1]   School of Aerospace and Automotive Engineering, Laboratory of renewable energies and advanced Materials (LERMA), L'Université Internationale de Rabat, Sala Aljadida, Rabat-Salé, 11100, Rabat, Morocco
[2]   Department of Mechanical Engineering, Faculty of Engineering, International Islamic University of Malaysia, Kuala Lumpur, Malaysia

ARTICLE INFO	ABSTRACT
  	The Micro Aerial Vehicles (MAVs) operate at a critical range of low Reynolds number (Re). The implementation of the low (Re) aerodynamics for MAVs has brought interest into the study of high-lift low Re airfoils. Such investigations may bring new insight into the aerodynamic performance of MAVs flights. The aim of the current investigation is to exam different numerical methods in the aerodynamics prediction of high-lift low Reynolds number S1223 airfoil. For that purpose, the Spallart Allmaras (S-A), two equations SST K-ω and the four equations transition γ-Reθ SST turbulence models were used. Results revealed that the SA turbulence model can predict the pre-stall low angles of attack and provides a good agreement with experimental data and XFOIL results. Whereas the two-equation model SST-enhanced K-ω and the transition SST models predict better the unsteadiness of the stall behaviour. XFoil accurately predicts the highest lift coefficient, even if it occurs at a lower angle of attack. These results showed the promising ability of the transition SST selection in predicting the stall behaviour.

1. Introduction

Unmanned aerial vehicles (UAVs) and micro aerial vehicles (MAVs) fly at flight conditions of low Reynolds number (Re). The improvement of the MAV aerodynamic efficiency requires aerodynamicists to increase their study attention to fixed-wing section (airfoil) aerodynamics [1].

The accuracy and the resilience of numerical approaches are essentially need a proper industrial turbulence model, therefore, yet many low-Reynolds solutions could not be achieved.

The low Reynolds number flow is known for the early appearance of separation bubbles. The numerical methods using the computational fluid dynamics (CFD) techniques showed difficulties in capturing the separation location over the suction surface of the airfoil. The flow at a low Reynolds number is also known to be in transition from laminar to turbulent [2].

Several studies have explored flow aerodynamics behaviour at low Reynolds number and a few studies have examined the selection of turbulence models.

Such a computation has been carried out by Morgado *et al.,* [3] in which they compared various turbulence models using CFD commercial codes and question their capability to capture the transition behaviour over high lift airfoils. By comparison to XFOIL, they used Shear Stress Transport (SST) k −ω and k − kl −ω transition models for performance predictions of low Reynolds number high lift airfoils, mainly E387 and S1223 airfoils. Their results showed the challenges to CFD turbulence models in better computing airfoil performance data.

A comparison study of various turbulence models by Aftab *et al.,* [4] to test the flow simulation capabilities at Re number of 120,000. They tested Spallart Allmars (S-A), two-equation SST K-ω, three equation Intermittency (γ) SST, k-kl-ω and the four-equation transition γ-Re$_\theta$ SST. They concluded that the γ -Re SST is the model that accurately predicts flow behaviour at both low and high AoA.

Similarly, Khoo [5] investigated the flow transitions over FX63-137 airfoil by Wortmann [6] using high order four-equation transition SST to capture the flow transitions at low Reynolds numbers. The predicted onset of separation agrees well with the experimental measurements. Another method for addressing the separation bubble structure is described by Che Ibrahim and Abdullah [7] and showed that this separation phenomenon directly affects the aerodynamic performance.

The effect of transitions in the prediction of flow characteristics has not been studied extensively. The transitional turbulence models are used in the prediction of the transitions over airfoils operating at low Re. It emphasizes the behaviour of separation bubbles and the strong 3D nature of the flow as surveyed by Wauters *et al.,* [2]. In their survey work, they explored transitional turbulence modeling from the perspective of small UAVs and concluded that there is still a need for an accurate turbulence model able to capture the transition behaviour for low Reynolds numbers of flows. Table 1 summarizes the possible selection of the turbulence models for Low Re number flows.

The high lift S1223 airfoil at low-Reynolds number has been designed by Selig and Guglielmo [8,9] and tested experimentally at a Re number of $2x10^5$. Jameel *et al.,* [10] designed a bio-like UAV model based on Corvus Splendens using S1223 airfoil for the wing section which has the capability to operate at fairly low altitudes as well as performs equally for low and high speeds.

The use of the 3-equation Intermittency SST model in the numerical investigation by Zohary *et al.,* [11] has displayed that unsteady simulation can predict transition with relatively good accuracy when compared to XFOIL. The S1223 airfoil excels in delivering a high lift coefficient compared to other profiles.

In the present study, a numerical investigation of the capability of various turbulence models to accurately predict the turbulent flow over the S1223 airfoil is conducted. The flow is considered as two-dimensional, steady and incompressible. The aerodynamic characteristics were evaluated at various angles of attack.

The general goal of this work is to examine different turbulence models used at low Reynolds number. The capability of the Spalart Almaras (SA) [12], SST-K-ϖ- [13], and Transition SST [14] turbulence models in capturing the separation point and stall behaviour of the S1223 airfoil is tested. The current numerical study was carried out using ANSYS Fluent commercial CFD code. The obtained numerical results are compared to the potential flow analysis using XFoil code and experimental data.

Table 1
Summary of the selection of turbulence models

Ref	Method	Re	Findings
Zohary et al., [11]	Intermittency SST model	0.3×10^6	The model can predict transition with relatively good accuracy. S1223 excels at providing high lift at the cost of increased drag.
Xia *et al.,*[15]	Review	10^4-10^6	Deviation in data increases with decrease in the Reynolds number and available tools of simulation face difficulties to predict it accurately.
Dong *et al.,* [5]	Transition SST & experiment	0.3×10^6 0.5×10^6	Good agreement between Exp and simulations regarding separation and re-attachment and the (high lift FX 63-137) aerodynamic coefficients.
Wauters *et al.,* [2]	K-ω, SST K-ω, k-kl-ω and SST.	-	There has yet to be discovered a universally successful model. On the predictive qualities, it is difficult to reach a clear conclusion.
Aftab *et al.,*[4]	(S-A), SST K-ω, k-kl-ω and SST.	0.12×10^6	SST is the chosen model because it accurately predicts flow behaviour at low and high AoA in a short amount of time.

2. Methodology
2.1 Mathematical Models

The model (S-A) [12] is a one-equation model (Eq.(1)) that solves the transport equation of the turbulent kinematic viscosity $\tilde{v}$ and is written as:

$$\frac{D\tilde{v}}{Dt} = c_{b1}\left[1 - f_{t2}\right]\tilde{S}\tilde{v} + \frac{1}{\sigma}\left[\nabla.\left((v + \tilde{v})\nabla\tilde{v}\right) + c_{b2}\left(\nabla\tilde{v}\right)^2\right] - \left[c_{\omega1}f_\omega - \frac{c_{b1}}{k^2}f_{t2}\right]\left[\frac{\tilde{v}}{d}\right]^2 + f_{t1}\Delta U^2 \tag{1}$$

Then, the *turbulent eddy viscosity* is determined using the following:

$$\mu_t = \rho\tilde{v}f_{v1} \quad . \quad f_{v1} = \frac{\chi^3}{\chi^3 + c_{v1}^3} \quad . \quad \chi = \frac{\tilde{v}}{v}$$

The Shear Stress Transport (SST) k −ω model of Menter [13] is also chosen in aerodynamics applications for the low Reynolds number flows. The model is a two-equation eddy-viscosity closure (Eq. (2,3)):

$$\frac{D(\rho k)}{Dt} = \tau_{ij}\frac{\partial u_i}{\partial x_j} - \beta^*\rho\omega k + \frac{\partial}{\partial x_j}\left[\left(\mu + \sigma_k\mu_t\right)\frac{\partial k}{\partial x_j}\right] \tag{2}$$

$$\frac{D(\rho\omega)}{Dt} = \frac{\gamma}{v_t}\tau_{ij}\frac{\partial u_i}{\partial x_j} - \beta^*\rho\omega^2 + \frac{\partial}{\partial x_j}\left[(\mu+\sigma_\omega\mu_t)\frac{\partial\omega}{\partial x_j}\right] + 2(1-F_1)\frac{\rho\sigma_{\omega2}}{\omega}\frac{\partial k}{\partial x_j}\frac{\partial\omega}{\partial x_j} \tag{3}$$

And the turbulent eddy viscosity is defined in k −ω:

$$\mu_t = \frac{\rho a_1 k}{\max(a_1\omega,\Omega F_2)}$$

Langtry and Menter [14] afterward developed the two-equation Menter model for transition modelling by adding two more equations. One for intermittency γ (Eq. (4)) and one for a transition Re_θ (Eq. (5)). The transition SST is also known as the "gamma-Re-theta-SST" model:

$$\frac{D(\rho\gamma)}{Dt} = P_\gamma - E_\gamma + \frac{\partial}{\partial x_j}\left[\left(\mu+\frac{\mu_t}{\sigma_f}\right)\frac{\partial\gamma}{\partial x_j}\right] \tag{4}$$

Where the sources of transition are stated as follows:

$$P_\gamma = F_{lengthh}c_{a1}\rho S[\gamma F_{onset}]^{0.5}(1-c_{e1}\gamma)$$

And $E_\gamma = c_{a2}\rho\Omega\gamma F_{turb}(c_{e2}\gamma-1)$

$$\frac{D(\rho\tilde{\mathrm{Re}}_{\theta t})}{Dt} = P_{\theta t} + \frac{\partial}{\partial x_j}\left[\sigma_{\theta t}(\mu+\mu_t)\frac{\partial\tilde{\mathrm{Re}}_{\theta t}}{\partial x_j}\right] \tag{5}$$

Where the source term is defined as follows:

$$P_{\theta t} = c_{\theta t}\frac{\rho}{T}\left(\mathrm{Re}_{\theta t}^{eq} - \tilde{\mathrm{Re}}_{\theta t}\right)(1-F_{\theta t})$$
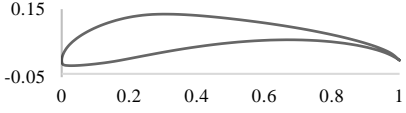
2.2 Material

The design idea of the S1223 airfoil aims to combine the beneficial recovery concave pressure effect with a high lift at a low Reynolds number of 200,000. S1223 airfoil was constructed in the University of Illinois at Urbana-Champaign (UIUC) subsonic wind tunnel by Selig and Guglielmo [9]. Table 2 illustrates the S1223 airfoil parametrization.

As the first stage of this study, the high-lift S1223 airfoil with available experimental data was adopted. The numerical simulation was conducted using the ANSYS Fluent CFD commercial code for validation purposes. The validation was performed by comparing three turbulence models to examine their capability of capturing the aerodynamic stall and the characteristics of the flow around the S1223 airfoil. The three turbulence models were compared with the S1223 airfoil available experimental data [9].

Table 2
Airfoil parametrization

S1223 airfoil profile	Thickness		Camber		L.E Radius
	12.1283% C	At X/c=21.05	8.67%	At x/c=49.05	3.56% C

2.3 Grid Generation

To establish the effects of the mesh and the number of elements in it, a sensitivity analysis was performed. Further, an extensive simulation of the flow field over S1223 airfoil was conducted to test the sensitivity of the turbulence models.

The ICEM CFD, ANSYS tool for hexahedral mesh generation was used to create a C-H-type grid around the airfoil. A high-structured mesh was generated and shown in Figure 1. A reasonable number of elements that enable an efficient flow field illustration around the airfoil were used. The grid independence study indicates that a 115000 with a Y^+ value set to 0.8 element is sufficient for the flow simulation and the lift coefficient values have no noticeable change beyond this element number as shown in Figure 2. The numerical values of the S1223 airfoil aerodynamic characteristics at different AoA will be compared to the experimental values in the next sections.
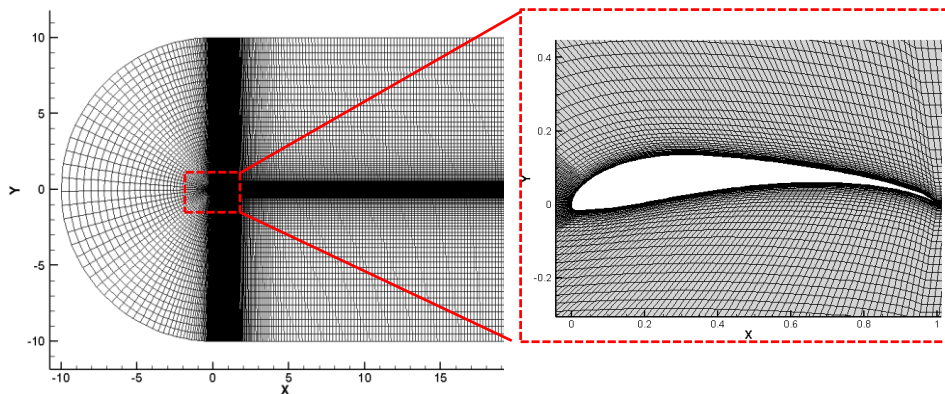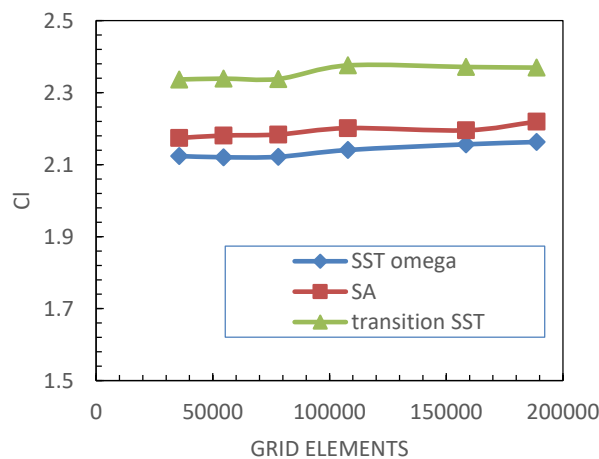

Fig. 1. Mesh of fluid domain around the airfoil

Fig. 2 Lift coefficient grid Independence analysis

3. Results

3.1 Aerodynamic Characteristics

Aerodynamic forces coefficients acting on the airfoil at different angles of attack are to be predicted and analyzed. For that reason, the flow over S1223 airfoil was simulated using Spalart-Allmaras (SA), enhanced SST K-ω, and transition SST turbulence models.

The numerically predicted lift coefficient (Cl) of the S1223 airfoil is compared against the experimental data [9] as well as with potential flow XFoil code that combines the panel method and the integral boundary layer formulation [16]. Table 3 shows the error percentage of each model at the angle AoA= 12 and Re = 200,000 compared to the experimental value. The Transition SST shows good agreement with experimental data and XFoil results though its high computational cost.

Figure 3 shows the comparison of the lift coefficient of the turbulence models and the XFoil with experimental data. The S-A model seems to predict well the lift coefficient at the angle of attack less than stall angle of attack and has a good agreement with the experimental results as well as XFoil at that range of the angle of attack.

The S-A turbulence model and XFoil predict well the Cl_{Max} value compared to the experimental value. But S-A turbulence model fails to predict the aerodynamic characteristics after stall which is likely due to poor capability of this model in estimating the separation point. Whereas the SST-K-ω and transition SST capture the lift coefficient well from an angle equal to or higher than the stall angle of attack.

At high angles of attack, transition occur at low-Reynolds number and flow become unsteady. SST K-ω and Transition SST turbulence models were selected to capture the flow field properties and to account for the unsteady flow phenomenon.

The difficulty to obtain a better agreement with experimental data at an angle of attack beyond stall for the three studied turbulence models may be due to the three-dimensional effect as reported by Storms and Jang [17]. Also, may be due to limitation of the wind tunnel testing of airfoil at high angles of attack where the two-dimensional experiments are extremely difficult to achieve particularly at stall as stated by the NASA Langley Research Center of Turbulence Modelling Resource [18].

In other words, within the stall angle and beyond SA turbulence model fails to capture the transitions. Whereas the two-equation turbulence model SST K-ω and transition SST captured the unsteadiness of the dynamic stall well as shown in Figure 4. Lift and drag polar results show once again that SST-K-ω and Transition SST model results to be in close agreement with experimental data.

In terms of drag coefficient, the Transition SST model underestimates Cd values compared to the S-A, and K-ω SST which agree with XFoil results (Figure 5). This, in principle, can give rise to the lift to drag ratio as the Figure 6 presents. Where the aerodynamic efficiency is influenced by the prediction of the transition SST model.
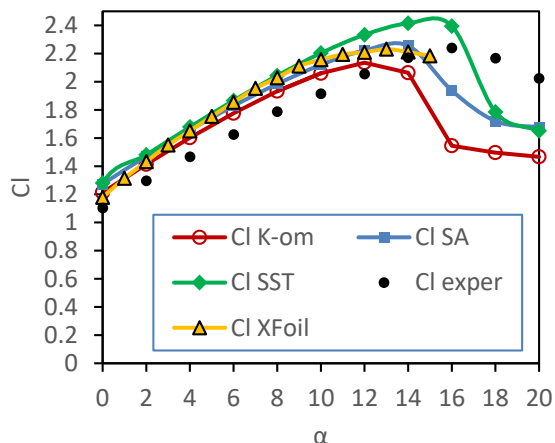
Fig. 3. Lift coefficient results of CFD, XFoil and experimental data
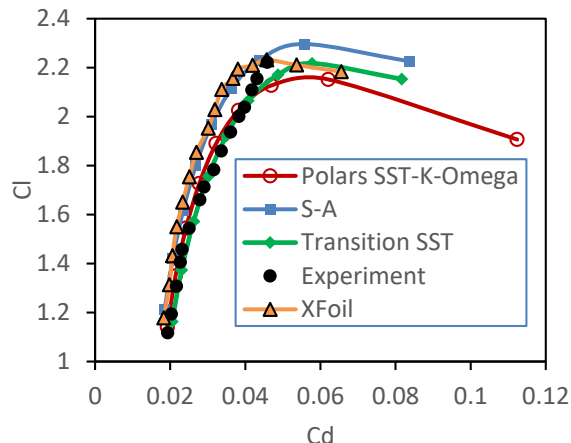

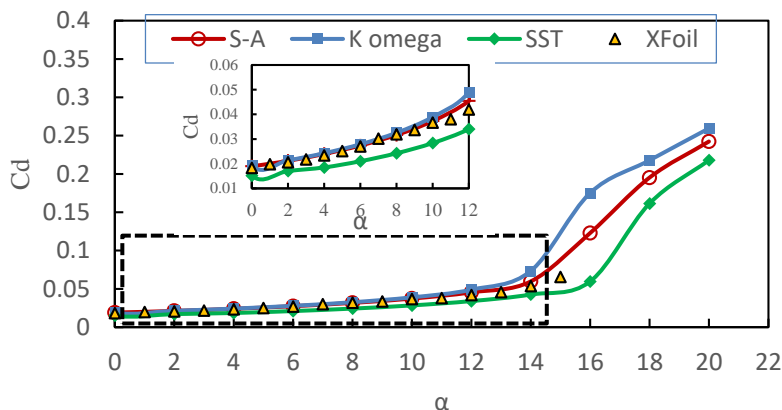**Fig. 4.** Lift and drag polars comparison of CFD, XFoil with experiment data
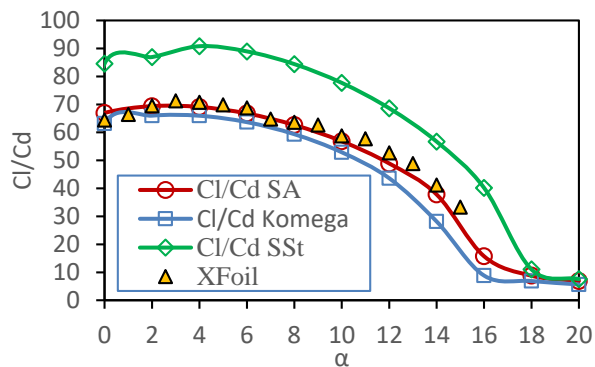

Fig. 5 Drag coefficient results of CFD, XFoil

Fig. 6 Aerodynamic efficiency (C/D) comparison

Table 3
Error calculated of the lift coefficient Cl as for 12°

Model	Cl	Error
Experimental	2.05	-
XFoil	2.21	7.2%
SA model	2.22	8.2%
K ω SST	2.14	4.3%
Transition SST	2.17	5.8%

3.2 Pressure Distributions and the Streamline Patterns

The pressure distribution, as well as the streamlines pattern over the airfoil at different angles of attack are shown in Figure 7 (a-c). In the streamlines trace, the appearance of the separation bubble is evident. At low angles of attack, the separation point is at 95% of chord length and a small bubble appears at the trailing edge (Figure 7a).

A larger separation bubble is observed during the stall conditions (Figure 7 b, c). With the increase in the angle of attack, the separation bubble has moved towards the airfoil leading-edge, and the separations take place at the mid of the chord length at an angle of attack of α= 14 as shown in Figure 7c.

A transition from laminar to turbulent flow and flow separation is seen clearly near the trailing edge of the airfoil where the transition to the turbulent flow is delayed causing shifting of the separation location to a point closer to the trailing edge.
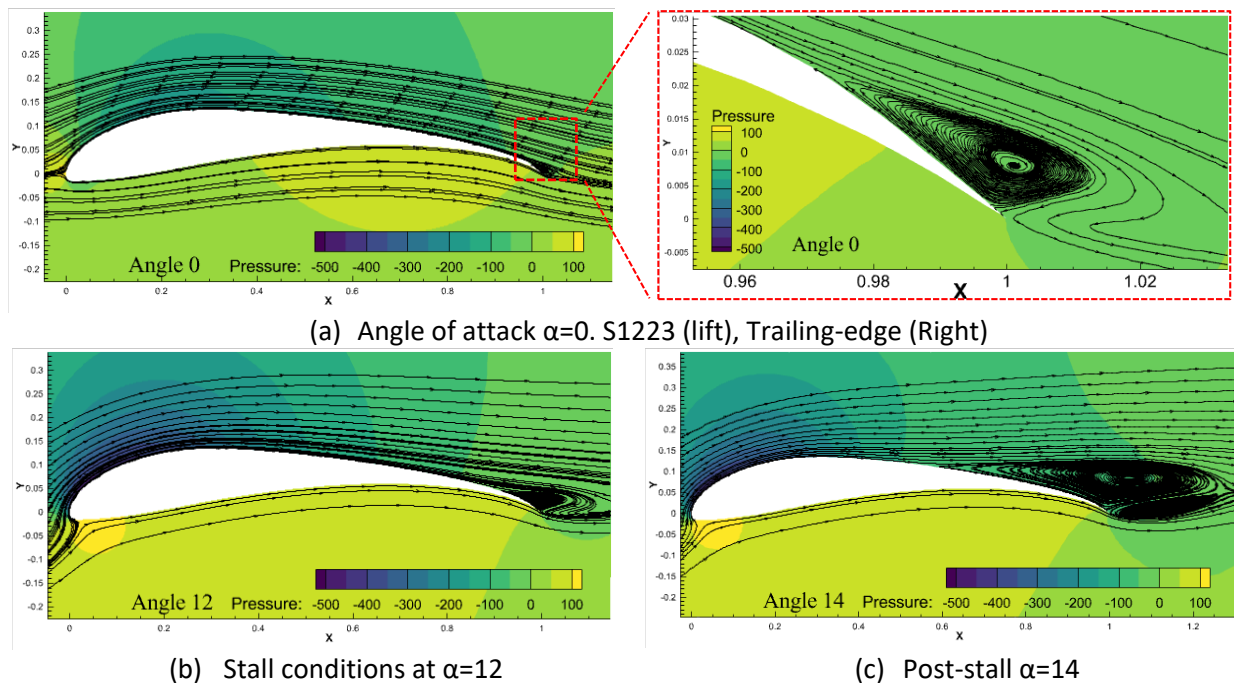

(a) Angle of attack α=0. S1223 (lift), Trailing-edge (Right)

(b) Stall conditions at α=12   (c) Post-stall α=14

Fig. 7. Streamlines and pressure distribution over S1223

Further comparison of the pressure coefficient of the studied turbulence models at angle of attack of 14° is shown in Figure 8. The difference in the upper surface pressure coefficient explains the differences in the lift coefficient prediction by the turbulence models compared to XFoil. The XFoil appears to predict the separation bubble.

The velocity profile vectors are used to emphasise the separation point over the airfoil at the stall angle conditions. The comparison of the prediction ability for the separation for the SST-K-ω and the Transition SST turbulence models are highlighted in Figure 9. The SST-K-ω model seems to predict the separations earlier than the SST Transition model. Early prediction of the separation is seen as indicated in the lift coefficient (Cl) curve in Figure 3 where the stall is seen early compared to the Transition SST model.
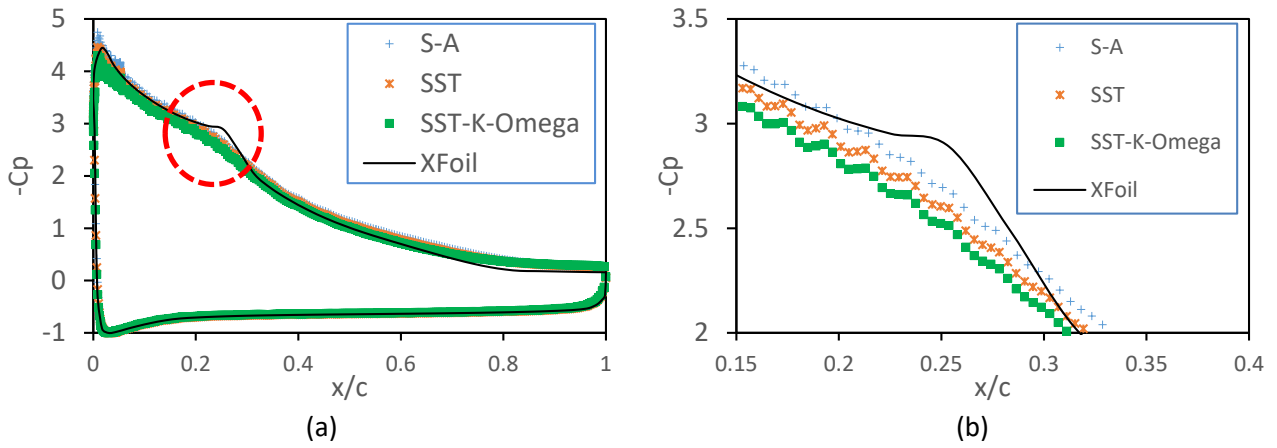
(a)

(b)

Fig. 8. Coefficient of pressure from the turbulence models. (a) Global variation of cp (b) Variation of cp near the separation region
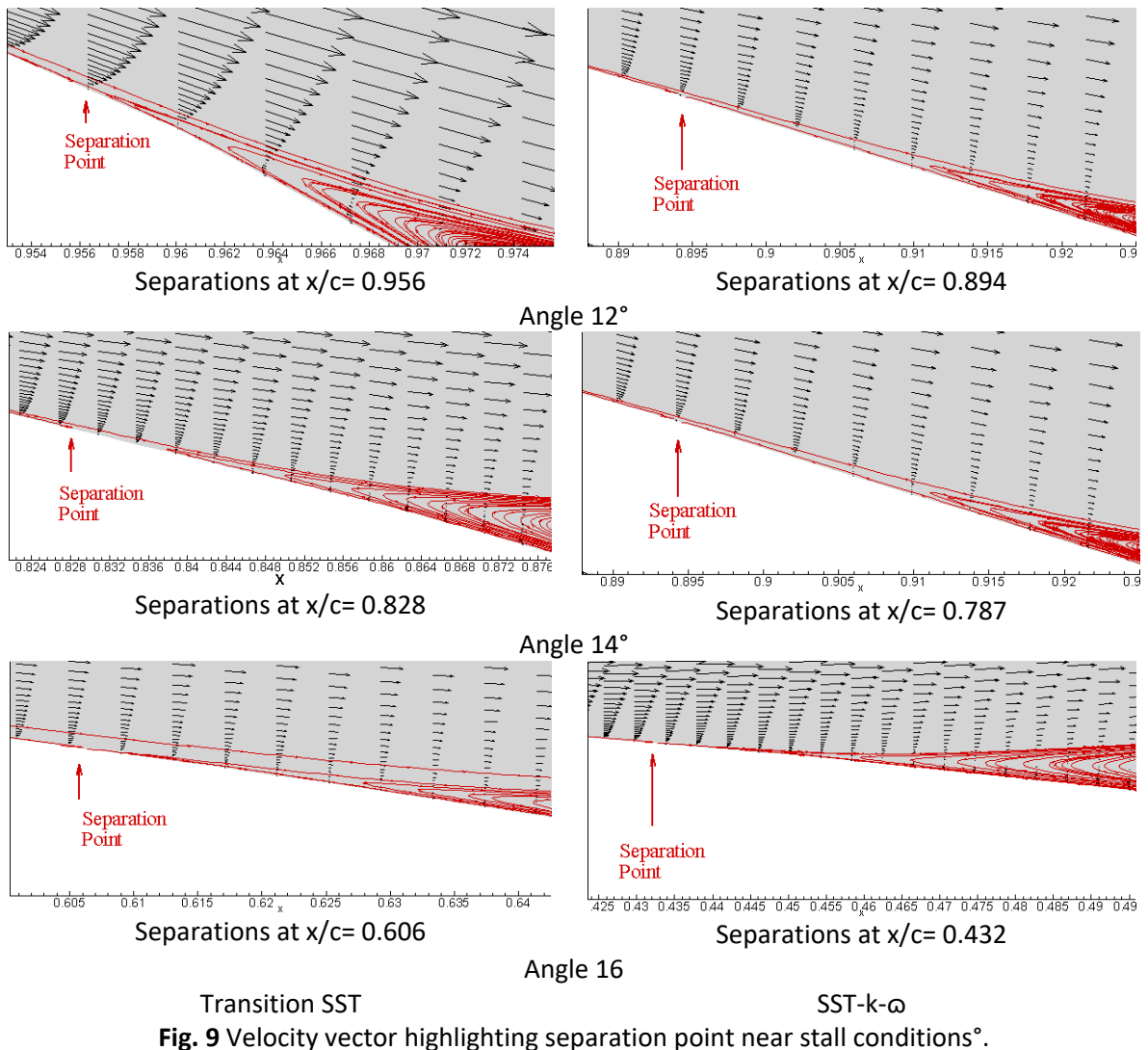

Separations at x/c= 0.956

Separations at x/c= 0.894

Angle 12°

Separations at x/c= 0.828

Separations at x/c= 0.787

Angle 14°

Separations at x/c= 0.606

Separations at x/c= 0.432

Angle 16

Transition SST   SST-k-ω

Fig. 9 Velocity vector highlighting separation point near stall conditions°.

4. Conclusions

The aerodynamic characteristics of high lift airfoils at low Reynolds number were investigated numerically using RANS and different turbulence models and XFoil. The results are compared to published experimental data. Three turbulence models mainly, the Spalart Almaras (S-A), K-ω SST, and Transition SST turbulence models were tested to examine their capability to predict the aerodynamic behaviour of the high lift low Re number airfoil. The three turbulence models show differences in capturing the separations near the stall conditions. The following are the observation of the study:

I.   Before stalling conditions is reached, the Spalart-Alamaras (S-A) turbulence model predictions of the lift and drag polar agree with experimental data and XFoil results. While after reaching the stall angle of attack, the SA fails to capture accurately the transition.

II.   Unsteady simulations of the SST-K-ω and the Transition SST turbulence models required a large computational time in comparison to the steady S-A turbulence model.

III.   Differences in the capability of estimating a separation point are one of the major explanations for the observed differences between the simulation approaches studied.

References
[1]   Michelson, R. C. Micro Air Vehicles. In *Handbook of Unmanned Aerial Vehicles* (K. P. Valavanis and G. J. Vachtsevanos, eds.), Springer Netherlands, Dordrecht, 2015, pp. 1305–1310.
[2]   Wauters, Jolan, and Joris Degroote. "On the study of transitional low-Reynolds number flows over airfoils operating at high angles of attack and their prediction using transitional turbulence models." Progress in Aerospace Sciences 103 (2018): 52-68. https://doi.org/10.1016/j.paerosci.2018.10.004.
[3]   Morgado, J., R. Vizinho, M. A. R. Silvestre, and J. C. Páscoa. "XFOIL vs CFD performance predictions for high lift low Reynolds number airfoils." Aerospace Science and Technology 52 (2016): 207-214. https://doi.org/10.1016/j.ast.2016.02.031.
[4]   Aftab, S. M. A., A. S. Mohd Rafie, N. A. Razak, and K. A. Ahmad. "Turbulence model selection for low Reynolds number flows." PloS one 11, no. 4 (2016): e0153755. https://doi.org/10.1371/journal.pone.0153755.
[5]   Dong, Hao, Tianyu Xia, Lin Chen, Shicheng Liu, Y. D. Cui, B. C. Khoo, and Aihong Zhao. "Study on flow separation and transition of the airfoil in low Reynolds number." Physics of Fluids 31, no. 10 (2019): 103601. https://doi.org/10.1063/1.5118736.
[6]   Wortmann, F. "The quest for high-lift." In 2nd International Symposium on the Technology and Science of Low Speed and Motorless Flight, p. 1018. 1974. https://doi.org/10.2514/6.1974-1018.
[7]   Ibrahim, Che Intan Hartini Che, and Aslam Abdullah. "Flow Topology around Low Reynolds Number Airfoils with Vortex Shedding." CFD Letters 12, no. 12 (2020): 85-103. https://doi.org/10.37934/cfdl.12.12.85103.
[8]   Selig, M. S., Guglielmo, J. J., Broeren, A. P., and Giguère, P. *Summary of Low Speed Airfoil Dara - Vol 1*. 1995.
[9]   Selig, Michael S., and James J. Guglielmo. "High-lift low Reynolds number airfoil design." Journal of aircraft 34, no. 1 (1997): 72-79. https://doi.org/10.2514/2.2137.
[10] Jameel, A., S. Khalid, M. Khan, K. Kamal, A. Aqeel, S. Mathavan, T. Awais, and T. Zafar. "A Bio inspired UAV model based on Corvus Splendens." In 2015 International Conference on Fluid Power and Mechatronics (FPM), pp. 797-802. IEEE, 2015.
[11] Zohary, Aideal Czar, Waqar Asrar, and Mohammed Aldheeb. "Numerical Investigation on the Pressure Drag of Some Low-Speed Airfoils for UAV Application." CFD Letters 13, no. 2 (2021): 29-48. https://doi.org/10.37934/cfdl.13.2.2948.
[12] SPALART, P., and ALLMARAS, S. A One-Equation Turbulence Model for Aerodynamic Flows. 1992.
[13] Menter, Florian R. "Two-equation eddy-viscosity turbulence models for engineering applications." AIAA journal 32, no. 8 (1994): 1598-1605. https://doi.org/10.2514/3.12149.

[14] Langtry, Robin B., and Florian R. Menter. "Correlation-based transition modeling for unstructured parallelized computational fluid dynamics codes." AIAA journal 47, no. 12 (2009): 2894-2906. https://doi.org/10.2514/1.42362.

[15] Xia, Tianyu, Hao Dong, Liming Yang, Shicheng Liu, and Zhou Jin. "Investigation on flow structure and aerodynamic characteristics over an airfoil at low Reynolds number—A review." AIP Advances 11, no. 5 (2021): 050701. https://doi.org/10.1063/5.0044717.

[16] Drela, M. XFOIL: An Analysis and Design System for Low Reynolds Number Airfoils. In *Low Reynolds Number Aerodynamics. Proc. Conf., Notre Dame, U.S.a., June 5-7, 1989 }Edited By T.J. Mueller]. (Lecture Notes in*, 1989, pp. 1–12.

[17] Storms, Bruce L., and Cory S. Jang. "Lift enhancement of an airfoil using a Gurney flap and vortex generators." Journal of Aircraft 31, no. 3 (1994): 542-547. https://doi.org/10.2514/3.46528.

[18] Turbulence Modeling Resource. *Langley Research Center Turbulence Modeling Resource*. 10. Volume 45, 1–8. https://turbmodels.larc.nasa.gov/naca0012_val.html. Accessed Mar. 2, 2021.